Exploiting Near-Field Coupling between Closely Spaced, Gas-Phase, 10 ± 5 nm Ag Nanoparticles Deposited on NaCl To Observe the Quadrupolar Surface Plasmon Absorption

David B. Pedersen* and Shiliang Wang

Defence R&D Canada−Suffield, Suffield, Alberta, T1A 8K6, Canada

Matthew F. Paige and Adam F. G. Leontowich

Chemistry Department, University of Saskatchewan, Saskatoon, Saskatchewan, S7N 5C9, Canada

Received: October 23, 2006; In Final Form: February 12, 2007

Ag nanoparticles with a diameter of 10 ± 5 nm were generated in the gas phase by using a sputtering/aggregation source and deposited onto NaCl prisms. Internal reflection spectroscopy was utilized to acquire UV−vis spectra of the nanoparticles in situ as they were being deposited. As the deposition proceeded, the interparticle spacing decreased steadily to effectively zero (contact). When the interparticle spacing was in the ca. sub-10 nm range, near-field coupling between the particles caused an increase in the intensity of the quadrupolar absorption, relative to the dipolar one. The deposition of gas-phase nanoparticles onto NaCl allows the average interparticle spacing to be varied, even in the 0−10 nm region, which is beyond the resolution of lithography techniques. This is the region where near-field interparticle coupling effects are important. To our knowledge, these are the first absorption spectra of quadrupolar resonances in particles less than ∼40 nm in diameter.

1. Introduction

Coupling interactions between metallic nanoparticles are distance dependent phenomena that profoundly affect the extinction spectra of the particles by shifting spectral features as much as hundreds of nanometers and by manifesting the appearance and the disappearance of entire extinction bands. Dipole coupling occurs readily when the internanoparticle spacing is comparable to or less than the wavelength of peak absorbance of the surface plasmon resonance (SPR) associated with the nanoparticles. Several experiments have studied the coupling in detail, monitoring changes in the UV−vis absorption spectrum that occur as the distance between adjacent nanoparticles in arrays or aggregates is systematically varied.[1−12] The distance dependence of the dipole coupling is generally well behaved and a shift of the surface plasmon resonance to longer wavelengths as the interparticle separation decreases is typically observed. For ordered systems, shifts to the blue may occur, depending on the polarization of the light with respect to the orientation of the nanoparticles. These shifts are typically much smaller than the red shift.[13,14] Much of this behavior can be explained in terms of electrodynamic interactions between particles, the influence of which falls off as $1/r$, where r is the interparticle separation.[15] The electrostatic interactions between particles fall off as $1/r^3$ and have a much shorter range of influence. These interactions become important when the distance between particles is less than ∼10 nm. At these distances the influence of the high-field gradient (near field) near the surfaces of the particles becomes important. One indication of a strong near-field interaction is the appearance of a quadrupolar absorption in the extinction spectrum of the interacting particles.[16] Quadrupolar absorptions are frequently observed as lower wavelength shoulders on the main (dipolar) surface plasmon absorption.[17] Unlike the dipolar, quadrupolar absorption positions are predicted to change little with interparticle separation, up to the point of contact.[16] When there is contact between the particles, both dipolar and quadrupolar absorptions shift radically. When interparticle spacing is reduced further to negative values, effectively varying the extent of particle overlap, the intensities and positions of both dipolar and quadrupolar absorption bands change significantly.

Experimental approaches to studying the effect of interparticle separation on the optical properties of collections of nanoparticles include nanosphere and e-beam lithography techniques. At relatively long interparticle distances, comparable to the wavelength of peak absorbance of the SPR, experimental results agree with theory. A smooth shift of the SPR to longer wavelengths is observed as the interparticle distance is decreased.[1,2,4,6] Using e-beam lithography, Nurmikko and coworkers have also studied the "negative distance" regime, where the degree of overlap between particles was varied systematically.[1] They found that particle overlap effectively eliminates the dipole−dipole interaction. With particle overlap there is a dramatic change in the spectra, from that of the separated particles, that includes a large shift of the dipolar absorption and the appearance of a relatively large feature due to quadrupolar absorption by the overlapping particles. The dumbbell shape of the particle resulting from overlap of two particles is thought to enhance the probability of quadrupolar absorption. Both the dipolar and quadrupolar features shift to shorter wavelengths as the extent of particle overlap is increased, tending toward the spectrum expected of the single particle that results when there is full overlap. Interestingly, no spectral features characteristic of quadrupolar absorption were observed in the spectra of particles in contact (interparticle separation of zero) or in any of the spectra where particles were separated from each other. This result is somewhat at odds with theoretical

* Author to whom all correspondence should be addressed. E-mail david.pedersen@drdc-rddc.gc.ca.

10.1021/jp066942t CCC: $37.00
Published on Web 03/24/2007

results that predict the appearance of a quadrupolar absorption when interparticle separation decreases below ~10 nm.[16] The discrepancy may simply reflect the inherent limits of the e-beam technique, which has a resolution of approximately 10 nm. Accordingly, the e-beam approach is not appropriate for studying particles with separations in the contact to 10 nm range—the range where near-field effects are expected to be important.

Experimental examples of nanoparticle spectra containing quadrupolar absorptions have so far been restricted to relatively large nanoparticles. The absence of analogous spectra for smaller particles is due in part to the fact that the probability of quadrupolar excitation increases with nanoparticle size. Accordingly, we find no literature examples of spectra with quadrupolar features for any particles smaller than ~30 nm in diameter, with the possible exception of the work of Panigrahi et al.[18] In contrast, there are many examples of quadrupole spectra for larger particles. Perhaps the best example of size facilitating multipolar absorption is the recent allthepole paper where the dipolar, quadrupolar, hexapolar, and octupolar absorptions were all observable in the extinction spectrum of a relatively large particle (diameter of greater than 90 nm).[17] In light of the relatively low probability of quadrupolar excitation in smaller particles, near-field excitation and/or strong interparticle coupling is expected to be a general prerequisite for observation of such transitions. Oscillating a quadrupole on the surface of a nanoparticle requires imposing a field across the particle with a gradient comparable to the size of the particle. For smaller nanoparticles, this decay length is much shorter than the wavelength of light used to excite the surface plasmon. Accordingly, for particles with diameters much smaller than UV−vis wavelengths, near-field excitation is generally prerequisite for observation of quadrupolar absorptions. Theory shows quite clearly that, even though no quadrupolar absorption is observed with far field excitation, the quadrupolar absorption can be nearly as strong as the dipolar one when the nanoparticle is excited in the near field, even for particles as small as 20 nm in diameter.[19] A key way to enhance the near field is to position nanoparticles in close proximity, within ~10 nm of each other, so that they are coupled through the effects of the near field that resides near the surface of the particles as they interact with light.[5,16] By taking advantage of this coupling, the acquisition of spectra containing quadrupolar absorption features should be attainable for nanoparticles smaller than ~30 nm in diameter.

In this paper we describe the coupling of internal reflection spectroscopy with a gas-phase nanoparticle deposition technique that allows us to follow the coupling between nanoparticles that occurs as the average interparticle spacing is systematically decreased. We use internal reflection spectroscopy as a way of imposing a near field on nanoparticles via the evanescent field generated by reflecting light off a salt−vacuum or salt−air interface, on which nanoparticles have been deposited. This approach is found to enhance the quadrupolar absorption significantly. We use the deposition of naked gas-phase nanoparticles as a method of making nanoparticle coated substrates as it provides an avenue toward the assembly of very small nanostructures, the simplest of which are clusters. Key properties of the nanostructures synthesized this way include the fact that they are naked (free of surfactant, oxide, and adsorbed water) during the deposition/assembly process and the fact that relatively small nanoparticles can be made. The size of the nanoparticles can be varied by altering the source conditions. The gas phase approach also has the advantage that internanoparticle spacing should change smoothly as a function of deposition time from large distances to effectively zero (contact) as the particle density increases on the surface of the substrate. In this case, the evolution of extinction spectra can be monitored as the interparticle spacing passes through the 10−0 nm region where near-field effects are important. This is the region currently beyond the resolution limits of e-beam and similar lithography techniques. The gas-phase approach has the disadvantage that interparticle spacing and the spectra attained are the average of the ensemble. Nonetheless, the technique does afford an opportunity to study the evolution of spectra as the effect of near-field interactions with neighboring particles increases as the average interparticle separation decreases below 10 nm.

2. Experimental Section

Ag nanoparticles were generated in the gas phase by using an aggregation-type source (Mantis Nanogen). A schematic of the apparatus is shown in Figure 1. Briefly, a voltage (200−400 V, 200−300 mA) applied between an anode cap and a metal target, in the presence of a few milliTorr of Ar, sustained a plasma inside the region capped by the anode. Ar was introduced at a rate of 10−50 sccm (MKS 1179A mass flow controller) through a showerhead inlet directed at the anode cap and positioned immediately in front of the anode cap. The Ar gas flow could be augmented with a 0−20 sccm flow (MKS 1179A mass flow controller) of He, which could be introduced into the aggregation zone through a second gas inlet. Varying the flow of He and Ar allowed the size of nanoparticles generated by the source to be varied. Condensation of the plasma gas began once the plasma gas exited the plasma region, through a hole in the anode cap, and entered the first aggregation zone. The gas then expanded into the second aggregation zone, which was evacuated by a 500 L/s turbo pump (Varian V-550). The nanoparticles thus generated passed through an orifice into the sample chamber where a pressure of $<10^{-4}$ Torr was maintained during deposition by a 300 L/s turbo pump (Varian TV-301). The nanoparticles were deposited onto a NaCl prism (International Crystal Laboratories) positioned in the nanoparticle beam path. Light from a deuterium lamp (Mikropak DH-2000) was piped into the sample chamber through an optic fiber, passed through a collimating lens, through one side of the prism, was reflected, and left the sample chamber through a quartz window as shown in Figure 1. The reflected light was then collected by a second collimating lens and focused into another optic fiber that carried the light to the CCD array spectrometer (Ocean Optics-SD2000). The spectrometer was set to acquire spectra every 2−3 s during deposition so that spectra of the nanoparticles could be acquired in real time, as they were being deposited. Alternatively, the deposition was monitored in situ in transmission mode, where light exiting the optic fiber was passed directly through a NaCl spectroscopic window (replacing the salt prism), exited the chamber, then passed through the collimating lens and into the collection optic fiber of the SD2000 spectrometer. Deposition times varied from 30 s to 15 min for different samples. Analogous spectra were collected outside of the chamber in air. For some samples, spectra were first acquired in ATR (internal reflection) mode by using the NaCl prisms, as described. The backsides of the prisms were then filed down thus making a NaCl window ~$^1/_4$ in. thick. The filed side was then water polished. The window was then placed between the source and detection fiber optics of the SD2000 spectrometer and a transmission spectrum acquired. In this way, ATR and transmission spectra of the same sample could be collected, once.

Atomic force microscope (AFM) images of nanoparticle coated NaCl prisms were collected with use of a Dimension

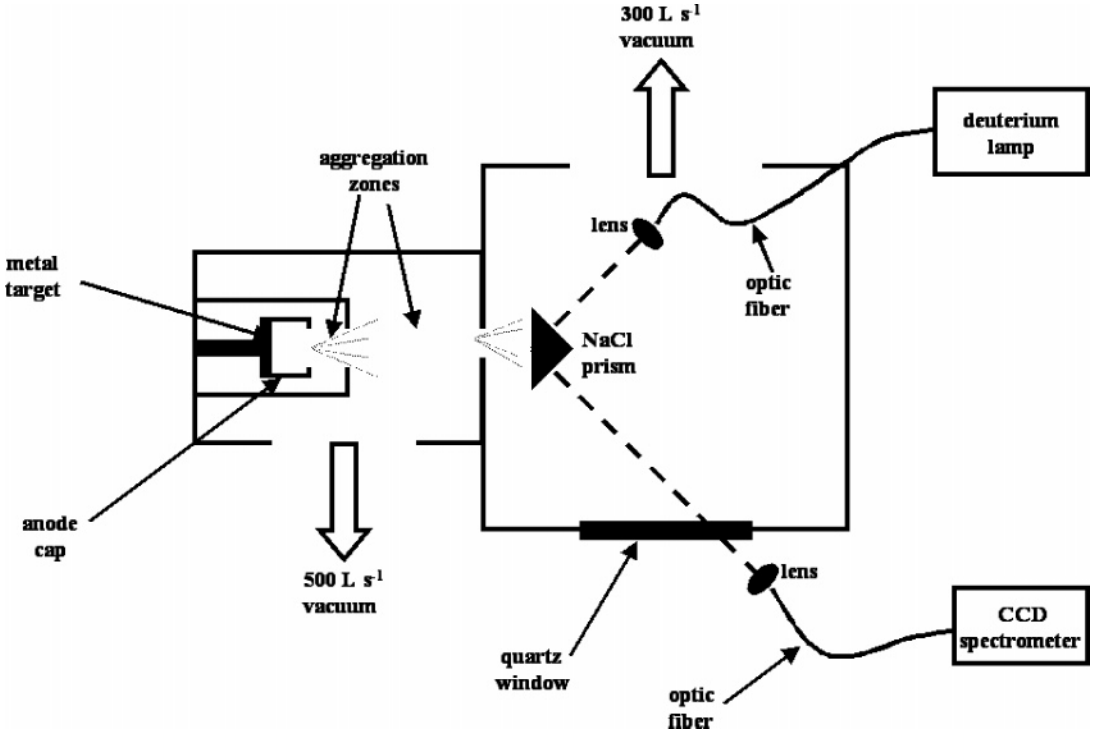

Figure 1. Schematic of the apparatus used to generate gas-phase Ag nanoparticles and deposit them onto NaCl substrates. The spectrometer allows the deposition process to be monitored in real time. The main chamber is nominally 1 ft^3 (2.7×10^4 cm^3) in volume. See text for details.

Hybrid Nanoscopic system operating in intermittent contact ("tapping") mode, in air. The microscope was mounted in an acoustic-vibration isolation system to minimize vibrational noise in the measurments. Commercial silicon AFM probes (Veeco Metrology Group, Santa Barbara, CA), with nominal spring constants of 42 N m^{-1}, were used for the measurements. The NaCl prism surfaces could be imaged repeatedly without damaging the substrate surface or moving nanoparticles with the tip. Nanoparticle diameters were determined by measuring the height of the particle above the substrate surface.

3. Results

Sample spectra of the gas-phase Ag nanoparticles deposited onto a NaCl prism are shown in Figure 2. In transmission mode, where light passes through the nanoparticle sample during acquisition of the spectrum, a single absorption feature characteristic of the surface plasmon resonance of Ag nanoparticles is observed at 470 nm. In reflection mode, where light is reflected off the back of the nanoparticle sample during acquisition of the spectrum, two bands are observable: the SPR band at 470 nm and a second band at 375 nm. The two spectra shown in Figure 2 are of the *same sample* (10 min deposition time) and the differences in the spectra are due to differences in the way the spectra were acquired (i.e., transmission vs reflection modes).

The band at 375 nm was found to increase in size relative to the SPR band with deposition. Acquiring spectra in situ as Ag nanoparticles were being deposited onto a NaCl prism in the vacuum system allowed the growth of this band to be monitored. As seen in Figure 3, at low deposition times the 375 nm band was not visible. At longer deposition times the band can be seen—clearly at the longest deposition time. At later times the band can become comparable in size to the SPR band, as is the case in Figure 2. It is also a noteworthy general observation that this band does not shift significantly as the deposition

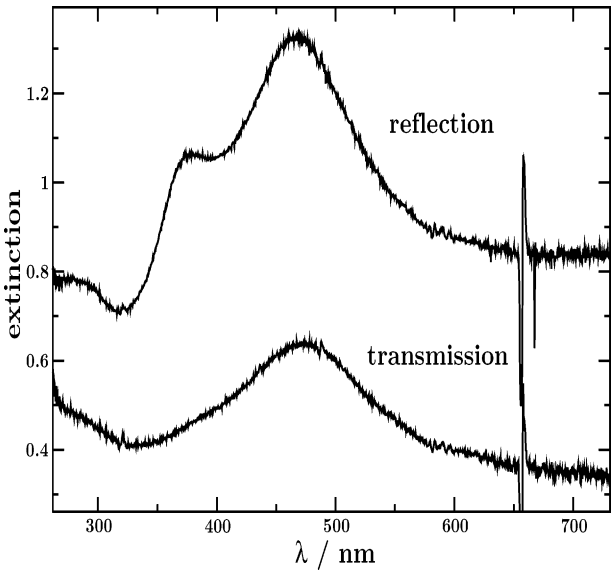

Figure 2. Two spectra of the same sample of Ag nanoparticles deposited on NaCl. The upper spectrum is a reflection spectrum taken by internally reflecting the light off the surface on which the nanoparticles were deposited. The lower is a transmission spectrum taken by passing light through the sample. λ denotes wavelength.

proceeds. Changing the size of nanoparticles is known to cause both the dipolar and multipolar absorptions to shift, opposite to what is observed. So the appearance and growth of the 375 nm band cannot be attributed to an increase in the average size of the nanoparticles. The lack of shifting of the 375 nm band is also different from that of the band originally near 400 nm, which shifted approximately 100 nm in going from the short to long deposition times as shown in Figure 3. The extent of shifting of the latter band is more clearly illustrated in Figure 4 where the peak position is plotted as a function of deposition time. These data are from internal reflection spectra acquired in situ during deposition of the Ag nanoparticles onto the NaCl

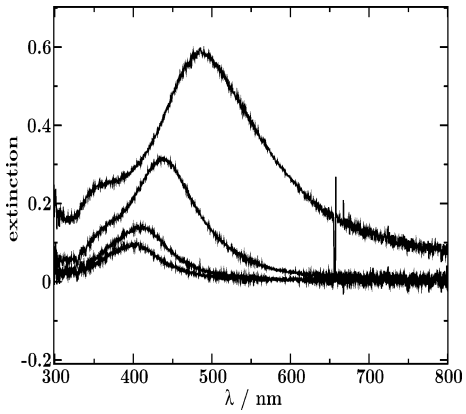

Figure 3. Absorption (extinction) spectra of Ag nanoparticles on a NaCl substrate. These spectra were collected in situ as the nanoparticles were being deposited. A time series is shown with the lower spectrum being acquired early in the deposition (125 s), the uppermost later (500 s), and the others at times in-between (150 and 250 s, respectively). The feature near 375 nm is the quadrupolar absorption (see text). λ denotes wavelength.

prism substrates. Data for a number of nanoparticle samples are shown and for all of them the absorption band is seen to steadily shift to longer wavelengths as the deposition proceeds. At longer deposition times the curves level off, likely due to primary coupling effects being complete, as noted in an earlier publication.[20]

The ~375 and ~450 nm bands were also found to respond differently to changes in the angle of reflection used when acquiring the internal reflection spectra. In Figure 5, spectra of a sample of Ag nanoparticles on a NaCl prism are shown. Each spectrum corresponds to a different incident angle, the angle the light makes with the surface as it reflects off the back of the nanoparticles that are deposited on the hypotenuse face of the NaCl prism. As seen, changing the angle has a profound effect on the relative intensities of the ~375 and ~450 nm absorption bands. At 54.7° the shorter wavelength band is seen to be more intense than the longer. There is also an offset of the baseline at longer wavelengths that becomes more pronounced as the critical angle (53.6°) is approached. This effect is caused by violation of the internal reflection condition at these wavelengths (i.e., above ~575 nm) due to the wavelength-dependent nature of the refractive index of NaCl. The different responses of the ~375 and ~450 nm bands suggest that the mode of absorption is different for the two bands.

A sample AFM image of Ag nanoparticles deposited onto NaCl is shown in the inset of Figure 6. The Ag nanoparticles are well dispersed and, as seen, each individual nanoparticle can be resolved. The nanoparticles shown in Figure 6 are found to be 10 ± 5 nm in diameter, which is typical of the images acquired. There are also some larger nanoparticles evident in the image. These are thought to result when a gas-phase Ag nanoparticle collides with a Ag nanoparticle sitting on the NaCl surface during the deposition process and coalescence of the two particles occurs. Consistent with this reasoning, the number of these larger particles was found to increase as the deposition proceeded. With increasing deposition time the number of particles on the NaCl surface increases and the probability of such a collision increases. The graph shown with the AFM image in Figure 6 illustrates the effect of interparticle distance on the position of the 450 nm (dipolar) absorption band. For these data, the average interparticle separation was determined from the AFM image and the peak position was determined from the internal reflection spectrum of the sample. Other data shown on the graph are scaled deposition data and theoretical data described further below.

4. Discussion

The effectiveness of near-field excitation as a means of circumventing the low probability of quadrupolar absorption in small nanoparticles is clearly illustrated in Figure 2. The two spectra shown are of *the same sample* (10 min deposition), yet differ markedly. The transmission spectrum consists of a single band with a peak near 475 nm characteristic of the surface plasmon resonance expected of nanoparticles of this size (10 ± 5 nm), albeit shifted to the red by coupling as discussed below. At the earliest deposition times, when interparticle coupling is at a minimum, the band appeared at ~380 nm (as is typical, see Figure 4), which is expected for Ag nanoparticles of this size.[21,22] In the reflection spectrum the surface plasmon band was also visible but accompanied by a second band that appeared at shorter wavelengths, near 375 nm. These results agree reasonably with theoretically predicted spectra of 22 nm radius Ag nanoparticles.[23] Those spectra have a dipolar absorption near 400 nm and a quadrupolar absorption near 375 nm that is enhanced by near-field excitation, analogous to the results shown in Figure 2. On the basis of this agreement, and the more global observation that quadrupolar absorptions generally appear as peaks blue-shifted from dipolar absorptions,[1,5,11,15,17,19,23−26] the ~375 nm feature can be assigned as that of the Ag nanoparticle quadrupolar absorption. In addition to the sensitivity to near-field excitation, the band displayed other behaviors characteristic of quadrupolar absorption. Unlike the SPR band, the feature near 375 nm always appeared at approximately the same wavelength, regardless of the particle density on the NaCl surface. Such insensitivity to the environment is the antithesis of SPR dipolar absorptions and a characteristic of quadrupolar ones. The appearance of the 375 nm band at longer deposition times and its growth as the deposition proceeds, as seen in Figure 3, are also behaviors expected of quadrupolar absorption. With decreasing interparticle separation the extent of near-field coupling between particles is expected to increase and enhance the quadrupolar absorption (see below). In light of these behaviors and the agreement with theory, it is clear that the feature near 375 nm is the quadrupolar absorption. To our knowledge, these are the first experimental spectra in support of the theoretical prediction,[23] that is, spectra of Ag nanoparticles as small as these (diameter $= 10 \pm 5$ nm) in which both quadrupolar and dipolar absorptions are observable.

Oscillating a quadrupole on the surface of a nanoparticle requires imposing a field gradient across the particle much shorter than the wavelength of light and is therefore well-known to be enhanced by near-field excitation.[19,27−29] Accordingly, varying the relative magnitudes of the near and far fields affords an opportunity to enhance the quadrupolar absorption relative to the dipolar one, which allows the bands to be distinguished. In ATR spectroscopy, this can be accomplished to some extent by varying the angle of incidence, which impacts the magnitude of the evanescent field (near field) present at the NaCl−air interface. The effect is illustrated in Figure 5 where, as the critical angle is approached, the quadrupolar absorbance (shoulder) increased relative to the dipolar one. The reason for the preferential increase in the quadrupolar absorption stems from the different dependences of the absorbances on the field strength. The magnitude of the dipolar absorbance is governed by the strength of the electric field imposed while the magnitude of the quadrupolar absorption is dependent on the gradient of the field. When the critical angle is approached the gradient of

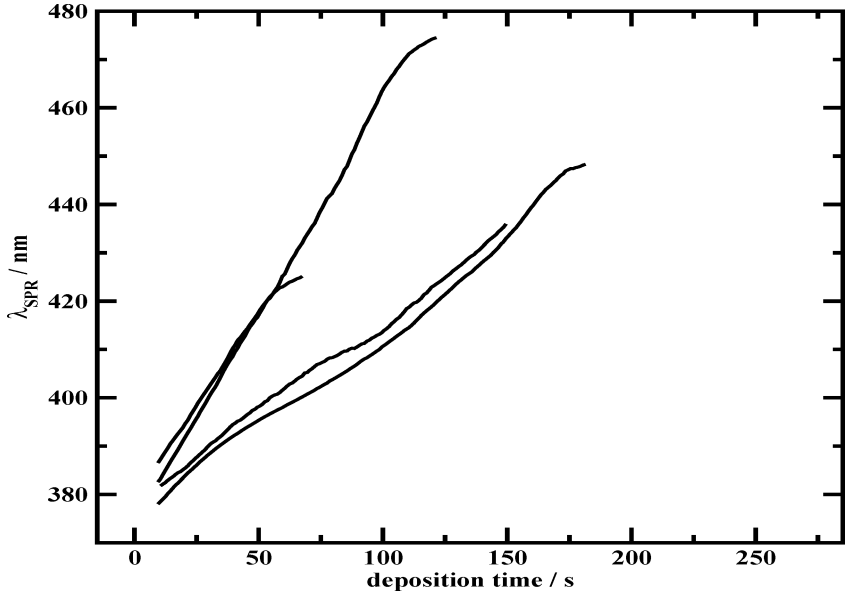

Figure 4. The SPR peak position (λ_{SPR}) of Ag nanoparticles on NaCl plotted as a function of deposition time. The different lines correspond to different nanoparticle samples deposited onto different NaCl substrates.

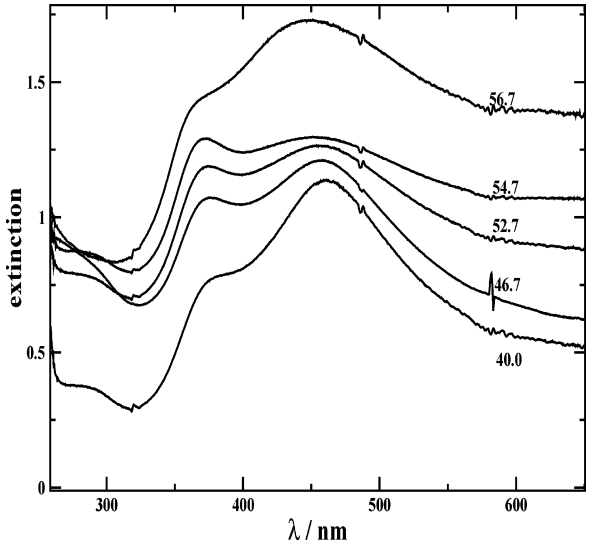

Figure 5. Spectra of Ag nanoparticles deposited on NaCl prisms acquired by using ATR spectroscopy. The incident angle used to acquire each spectrum is marked. The spectra have been vertically offset for clarity. λ denotes wavelength.

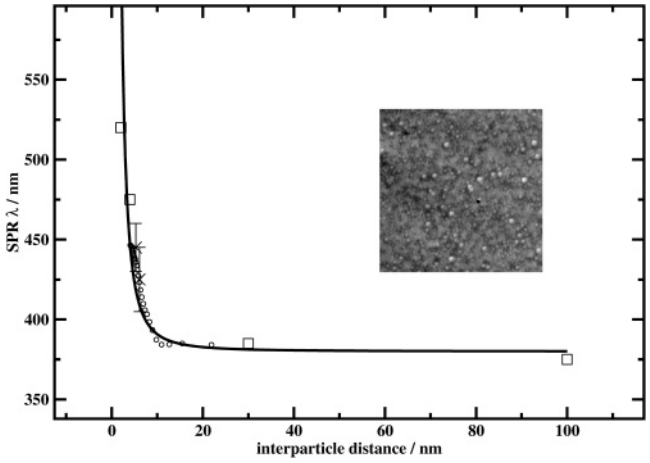

Figure 6. SPR position (dipolar absorption) shown as a function of interparticle separation. The large squares are the theoretical results of the Schatz group for 30 nm diameter nanoparticles.[16] The crosses with error bars are SPR wavelengths acquired for spectra where the average interparticle distance was determined via analysis of AFM images. The small circles are results of an experiment where the SPR peak position was measured as a function of deposition time, but the deposition time has been converted to distance (see text for details). The solid line is a fit of the data shown as a guide to the eye. The inset is a typical AFM image of Ag nanoparticles on a NaCl prism. The image is approximately 1 μm $\times$ 1 μm.

the field increases relative to the field strength itself and the quadrupolar absorption increases preferentially. The effect can be qualitatively modeled. Following Novotny and Hecht,[30] the strength of the evanescent field, at the plane of internal reflection, is proportional to the square of the Fresnal transmission coefficient, t_p^2. A plot of the calculated gradient of t_p^2 (∇t_p^2) ratioed to the field strength, t_p^2, is shown in Figure 7 as a function of the angle of reflection, Θ. ∇t_p^2 was determined by using the second-order finite differences method. As seen in Figure 7, the gradient increases dramatically, relative to the field strength itself, as the critical angle is approached. Accordingly, quadrupolar absorptions are expected to increase relative to dipolar ones, consistent with Figure 5. As a comparison, the ratios of the quadrupolar peak height to the dipolar peak height are plotted for different angles of incidence in Figure 7. There is reasonable agreement between the trend in the absorbance ratio and the predicted ∇t_p^2:t_p^2 (gradient:field strength) ratio. Furthermore, when acquiring spectra in transmission mode, with no internal reflection and thus no near-field effects, the quadrupolar absorption is not observed (see Figure 2) and the $abs_{quadrupole}$:abs_{dipole} ratio plotted in Figure 7 is effectively zero, which also agrees with the predicted trend in Figure 7 when far from the critical angle. Collectively, these results establish that by varying the angle of incidence of the excitation beam one can selectively excite the dipolar absorption exclusively, or one can enhance the quadrupolar absorption relative to the dipolar absorption. As the quadrupolar absorption stems from nanoparticles that are within the near field of neighboring particles, by tuning the incidence angle and thus the magnitude of the absorption, this population can be distinguished from that of the rest of the nanoparticles.

It is well-known that the extent of internanoparticle coupling can be systematically varied by changing the distance between

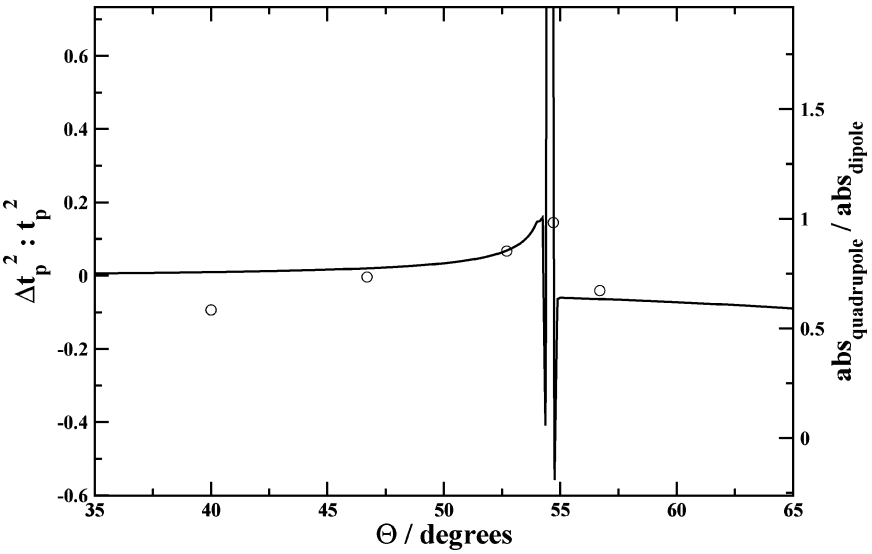

Figure 7. Graph of the quadrupolar:dipolar peak height ratio ($abs_{quadrupole}$:abs_{dipole}) plotted as a function of the angle of reflection used to acquire the ATR spectra. These experimental data are plotted as open circles and correspond to the right *y*-axis. The solid line is the theoretically predicted intensity ratio of the gradient of the intensity (∇t_p^2) to the intensity t_p^2 of the evanescent field generated at the nanoparticle coated NaCl−air interface off which the light was reflected. Calculation of ∇t_p^2:t_p^2 is described in the text. Θ is the angle of reflection.

neighboring particles. With the gas-phase deposition technique used, interparticle spacing decreases as the deposition time increases. The spray deposition method naturally deposits a collection of particles randomly oriented on the substrate surface. Accordingly, as the deposition proceeds the average interparticle distance systematically decreases as the probability of depositing one nanoparticle adjacent to another increases due to the increase in the coverage of the surface with nanoparticles. Mathematically, because the particle flux (number of particles per unit area per unit time) is constant, it is straightforward to show that the interparticle spacing should be proportional to $t^{-1/2}$, where t is the deposition time. Accordingly, the effects of increased coupling as deposition time increases are obvious in the spectra and include a steady shifting of the dipolar absorption to longer wavelengths. Sample data are shown in Figure 4 where the SPR position is plotted as a function of deposition time *t*. With the exception of longer times, where the leveling off of the SPR position indicates that all particles on the surface are coupled in the far field, the SPR position varies smoothly with *t*. This trend is that expected as the internanoparticle separation steadily decreases with deposition time.

As interparticle separation decreases as the deposition time is increased, the opportunity arises to compare the dipolar coupling observed in the spectra of deposited Ag nanoparticles with the theoretically predicted results of coupling between 30 nm Ag nanoparticles. The latter have been studied by the Schatz group and some of their results are plotted in Figure 6.[16] As seen, with decreasing interparticle separation, the SPR peak position shifts in an exponential manner to longer wavelengths. The SPR peak positions of some Ag nanoparticles deposited on NaCl prisms are also shown, superimposed over the theoretical results. For the experimental results, the average interparticle spacing was determined by using AFM images, a sample of which is shown in the inset in Figure 6. For a given distance (deposition time) different samples display slightly different SPR peak positions and these are reflected in the error bars shown. As seen, there is agreement between the experimental and theoretical results. A series of data points corresponding to the SPR peak position determined as a function of deposition time for a sample monitored in situ during the deposition is also shown in Figure 6. For these data, the experimental time values have been converted to effective distances by assuming that interparticle separation d is inversely proportional to the square root of deposition time ($d \propto t^{-1/2}$) and applying a scaling factor (i.e., $d = at^{-1/2}$). Qualitatively, the trend in the data agrees well with that predicted and with the other experimental data. The fact that the experimental trend mirrors the theoretical effectively confirms that experimentally the interparticle spacing decreases smoothly with deposition time and is proportional to $t^{-1/2}$. Consequently, the extent of interparticle coupling increases with deposition time. More importantly, there is good overall agreement between the results attained from the spectra of these small gas-phase-generated nanoparticles and the theoretical findings.

Theory predicts that near-field interactions between nanoparticles in close proximity significantly enhances the quadrupolar absorption of these particles. The results presented here clearly support these predictions. Having established that interparticle separation decreases with deposition time, it is clear that the growth of the quadrupolar absorption that occurs as the deposition proceeds correlates with the concurrent decrease in interparticle spacing. For near-field coupling to be effective, particles have to lie within ∼10 nm of each other.[16] An experimental example of the importance of near-field coupling for observation of multipolar absorptions comes from work on nanogold particles where spectra of particles separated by as little as 75 nm contained no quadrupolar absorption features even when near-field excitation (via reflection spectroscopy) was used.[6] The gas-phase deposition approach has no inherent limit preventing sub-10-nm proximity from being attained and it is clear from the AFM image in Figure 6 that many particle pairs within 10 nm of each other are in fact present on the nanoparticle-coated salt surface. The coalesced particles evident in the AFM image are larger particles expected to result when a gas-phase nanoparticle collides with a nanoparticle on the substrate surface and the two coalesce into one bigger nanoparticle comprised of two spatially overlapped nanoparticles. These particles may also contribute to the quadrupolar absorption observed but interparticle coupling is still expected to be prerequisite. It is unlikely, however, that these particles contribute significantly to the absorption. The variety of sizes of such particles, which varies with extent of overlap and number

of constituent particles, would likely manifest the appearance of quadrupolar absorptions at a variety of wavelengths in the spectra in contrast to observation.[1] Furthermore, previous work has shown that the dipolar absorption of coalesced particles is shifted markedly from that of the individual particles (as much as 150 nm for 30 nm high particles[1]), which would necessarily appear as an additional peak in the extinction spectrum, which is not observed. Accordingly, the quadrupolar absorption observed is that of individual 10 ± 5 nm particles coupled with their neighbors less than ~10 nm away through a near-field interaction. This result is somewhat in contrast with the work of Atay et al., where the quadrupolar absorptions were only observed for overlapping particles.[1] Our work clearly shows that overlap is not a prerequisite for observation of the quadrupolar absorbance even for very small nanoparticles. It also shows that the use of near-field excitation and interparticle coupling greatly facilitates observation of multipolar absorptions in such small particles.

5. Summary and Conclusions

The deposition of gas-phase nanoparticles onto substrates has been shown to be a novel approach to the study of multipolar absorptions of nanoparticles. The technique allows the average interparticle separation to be varied smoothly and simply by varying the deposition time. As the deposition proceeds, the observation of strong quadrupolar absorptions growing in the UV−vis spectra is clear evidence that the average interparticle separation has decreased below the ~10 nm limit where near-field coupling occurs. These results highlight one advantage of preforming nanoparticles in the gas phase and then depositing them onto substrates. It is possible by using this approach to assemble naked gas-phase nanoparticles with diameters on the order of a few nanometers into nanostructures smaller than those that can be made by other approaches. In contrast to e-beam and similar lithography techniques, the deposition approach is not inherently limited to ~10 nm resolution, and many particles within 10 nm of each other are produced during the deposition, as determined by AFM imaging. The nanoparticles are found to be $\sim 10 \pm 5$ nm in diameter, which are relatively small. To our knowledge, the spectra presented in this work are the first showing clear quadrupolar absorptions for such small nanoparticles. We have also demonstrated that, by varying the angle of reflection, the quadrupolar absorption can be enhanced significantly. This effect allows the population of near-field coupled nanoparticles to be distinguished from the rest of the population.

References and Notes

(1) Atay, T.; Song, J.-H.; Nurmikko, A. *Nano Lett.* **2004**, *4* (9), 1627−1631.

(2) Rechberger, W.; Hohenau, A.; Leitner, A.; Krenn, J. R.; Lamprecht, B.; Aussenegg, F. R. *Opt. Comm.* **2003**, *220*, 137−141.

(3) Haynes, C. L.; van Duyne, R. P. *J. Phys. Chem. B* **2001**, *105*, 5599−5611.

(4) Wei, Q. H.; Su, K. H.; Durant, S.; Zhang, X. *Nano Lett.* **2004**, *4* (6), 1067−1071.

(5) Malynych, S.; Chumanov, G. *J. Am. Chem. Soc.* **2003**, *125*, 2896−2898.

(6) Su, K. X.; Wei, Q. H.; Zhang, X.; Mock, J. J.; Smith, D. R.; Schultz, S. *Nano Lett.* **2003**, *3* (8), 1087−1090.

(7) Sandrock, M. L.; Foss, C. A. J. *J. Phys. Chem. B* **1999**, *103*, 11398−11406.

(8) Fort, E.; Ricolleau, C.; Sau-Pueyo, J. *Nano Lett.* **2003**, *3* (1), 65−67.

(9) Maier, S. A.; Brongersma, M. L.; Kik, P. G.; Atwater, H. A. *Phys. Rev. B* **2002**, *65*, 193408-1−193408-4.

(10) Bouhelier, A.; Bachelot, R.; Im, J.; Wiederrecht, G.; Lerondel, G.; Kostcheev, S.; Royer, P. *J. Phys. Chem. B* **2005**, *109* (8), 3195−3198.

(11) Haynes, C. L.; McFarland, A. D.; Zhao, L.; van Duyne, R. P.; Gunnarsson, L.; Prikulis, J.; Kasemo, B.; Kall, M. *J. Phys. Chem. B* **2003**, *107*, 7337−7342.

(12) Huang, W.; Qian, W.; El-Sayed, M. *J. Phys. Chem. B* **2005**, *109* (40), 18881−18888.

(13) Pinchuk, A.; Schatz, G. *Nanotechnology* **2005**, *16*, 2209−2217.

(14) Rechberger, W.; Hohenau, A.; Leitner, A.; Krenn, J. R.; Lamprecht, B.; Aussenegg, F. R. *Opt. Commun.* **2003**, *220* (1), 137−141.

(15) Zhao, L.; Kelly, K. L.; Schatz, G. C. *J. Phys. Chem. B* **2003**, *107*, 7343−7350.

(16) Jensen, T.; Kelly, L.; Lazarides, A.; Schatz, G. C. *J. Cluster Sci.* **1999**, *10* (2), 295−317.

(17) Kumbhar, A. S.; Kinnan, M. K.; Chumanov, G. *J. Am. Chem. Soc.* **2005**, *127*, 12444−12445.

(18) Panigrahi, S.; Praharaj, S.; Basu, S.; Ghosh, S. K.; Jana, S.; Pande, S.; Vo-Dinh, T.; Jiang, H.; Pal, T. *J. Phys. Chem. B* **2006**, *110*, 13436−13444.

(19) Bruzzone, S.; Malvaldi, M.; Arringhini, G. P.; Guidotti, C. *J. Phys. Chem. B* **2004**, *108*, 10853−10858.

(20) Pedersen, D. B.; Wang, S. *J. Phys. Chem. C* **2007**, *111*, 1261−1267.

(21) Liebsch, A. *Phys. Rev. B* **1993**, *48* (15), 11317−11328.

(22) Zhang, X.; Hicks, E. M.; Zhao, J.; Schatz, G. C.; Van Duyne, R. P. *Nano Lett.* **2005**, *5* (7), 1503−1507.

(23) Messinger, B. J.; von Raben, K. U.; Chang, R. K.; Barber, P. W. *Phys. Rev. B* **1981**, *24* (2), 649−657.

(24) Chumanov, G.; Sokolov, K.; Cotton, T. *J. Phys. Chem.* **1996**, *100* (13), 5166−5168.

(25) Evanoff, D.; White, R.; Chumanov, G. *J. Phys. Chem. B* **2004**, *108* (5), 1522−1524.

(26) Liz-Marzan, L.; Mulvaney, P. *J. Phys. Chem. B* **2003**, *107* (30), 7312−7326.

(27) Chaumet, P. C.; Rahmani, A.; de Fornel, F.; Dufour, J.-P. *Phys. Rev. B* **1998**, *58* (4), 2310−2315.

(28) Tojo, S.; Fujimoto, T.; Hasuo, M. *Phys. Rev. A* **2005**, *71* (1), 012507.

(29) Tojo, S.; Hasuo, M.; Fujimoto, T. *Phys. Rev. Lett.* **2004**, *92*, 053001.

(30) Novotny, L.; Hecht, B. *Principles of Nano-Optics*; Cambridge University Press: Cambridge, UK, 2006.